J Mol Model (2012) 18:2423–2431
DOI 10.1007/s00894-011-1250-x

ORIGINAL PAPER

Hydrogen storage in C_3Ti complex using quantum chemical methods and molecular dynamics simulations

Vijayanand Kalamse · Nitin Wadnerkar · Ajay Chaudhari

Received: 4 June 2011 / Accepted: 20 September 2011 / Published online: 12 October 2011

Abstract The hydrogen storage capacity of C_3Ti and C_3Ti^+ complex was studied using second order Møller-Plesset (MP2) and density functional theory (DFT) methods with different exchange and correlation functionals. Four and five H_2 molecules can be adsorbed on C_3Ti and C_3Ti^+ complex respectively at all the levels of theory used. This corresponds to the gravimetric H_2 uptake capacity of 8.77 and 10.73 wt % for the former and the latter respectively. The nature of interactions between different molecules in H_2 adsorbed complexes is also studied using many-body analysis approach. In the case of $C_3Ti(4H_2)$ complex, total five-body interactions is negligible whereas for $C_3Ti^+(5H_2)$ relaxation energy is negligible. All the many-body energies have significant contribution to the binding energy of a respective complex. Atom-centered density matrix propagation molecular dynamics simulations were carried out using different methods to confirm whether H_2 molecules remain adsorbed on C_3Ti and C_3Ti^+ complex at room temperature. Adsorption Gibbs free energies show that four and five H_2 molecule adsorption on C_3Ti and C_3Ti^+ at room temperature is energetically favorable and unfavorable respectively using MP2 as well as DFT methods used here. H_2 adsorption is thermodynamically favorable over a wide range of temperature on the C_3Ti than C_3Ti^+complex.

Keywords Adsorption energy · C_3Ti complex · DFT · Hydrogen storage · MP2 · Many-body analysis

V. Kalamse · N. Wadnerkar · A. Chaudhari (✉)
School of Physical Sciences,
Swami Ramanand Teerth Marathwada University,
Nanded 431606 Maharashtra, India
e-mail: ajaychau5@yahoo.com

Introduction

Hydrogen is a clean, abundant, non-toxic and renewable energy source. It has many advantages over fossil fuels and has an important application as an energy carrier in the automobile sector. Present natural energy sources in this sector are not only limited in their supply but also one of the factors causing global warming. To make hydrogen energy a perfect replacement for natural energy sources we need to overcome the problem of hydrogen storage [1, 2]. It is difficult to store hydrogen in gaseous and liquid form at ambient conditions. For commercialization of hydrogen energy, hydrogen storage at ambient thermodynamic conditions is essential. The materials capable of storing hydrogen with high gravimetric and volumetric density, operating under ambient thermodynamic conditions and exhibiting fast hydrogen adsorption-desorption kinetics are essential for the vehicular applications.

In recent years, several studies have been carried out to predict the hydrogen storage capacity of various materials. It includes the organic materials as well as metal- organic frameworks. Carbon based materials are considered because of their low molecular weight, high surface area and good mechanical properties. Transition metal atom decorated carbon nanostructures have attracted numerous attention for their hydrogen storing ability which includes nanotubes [3–13], buckyballs [14, 15], organometallic compounds [16, 17], metcars [18, 19] and polyacetylene [20] etc. Ti-decorated systems have attracted attention due to the unique Ti-H_2 interactions. It is possible that hydrogen adsorption on transition metal may affect the bond between transition metal and the base material. Hence, it is important to look at different structures where transition metal atom remains tightly bound to the system after H_2 adsorption. It would be interesting to study the hydrogen

adsorption properties of such Ti-C nanostructures. Hydrogen adsorption properties of such highly symmetric molecules like Ti_8C_{12} and $Ti_{13}C_{14}$ have been studied earlier [18, 19]. The rational behind selecting early transition metal atoms in transition metal decorated complexes is that they have less than half filled *d* shell which interacts with the antibonding orbital of H_2 molecule and as a consequence the H_2 bond gets slightly elongated after adsorption [21]. This results in molecular H_2 adsorption with adsorption energies lying between physisorption and chemisorption which is essential for the fast adsorption-desorption kinetics. Thus early transition metal containing complexes are more likely to be suitable as a host for hydrogen storage. An experimental study revealed that the ethylene-Ti complex can bind five H_2 molecules and clustering can also be avoided by making certain thickness of this complex in few nanometers [22]. This encourages us to study different materials which contains early transition metals specifically titanium.

In this paper, we have studied the structural and hydrogen adsorption properties of C_3Ti and C_3Ti^+ complex since such small molecules are basis of larger molecular assemblies. To date there are no detailed theoretical and experimental findings reported on C_3Ti in regard with hydrogen storage. Wang et. al. have reported vibrationally resolved photoelectron spectra of TiC_x clusters for x=2–5 [23] hence existence of such molecule is not questionable. In order to compare the results from the electron density based method viz. density functional theory (DFT) with those from the wave function based method, results from second order Møller-Plesset (MP2) method are included. The interaction of C_3Ti and C_3Ti^+ with H_2 molecules is studied here. MP2 and DFT method with different exchange and correlation functionals are employed for the calibration of hydrogen adsorption energies. As generalized gradient approximation (GGA) and hybrid-DFT cannot consider the Van der Waals interaction between H_2 molecule and the base material for hydrogen storage therefore MP2 and B97D methods are also included in this study [24]. Kinetic stability of the C_3Ti and C_3Ti^+ is studied by means of the gap between highest occupied molecular orbital and lowest unoccupied molecular orbital (HOMO-LUMO). Atom-centered density matrix propagation (ADMP) molecular dynamics (MD) simulations are also carried out at different levels for the accurate demonstration of hydrogen adsorption phenomenon. The isolated C_3Ti structure used here for hydrogen storage is lower in energy than the linear C_3Ti structure. Wang et al. suggested a ring type structure for C_3Ti in their interpretation which is confirmed by our study [23]. This paper is composed as follows: Computational details are given in the next section followed by the section Results and Discussion. Conclusions are drawn in the final segment.

Computational details

The geometries of $C_3Ti(nH_2)$ (n=1–4) and $C_3Ti^+(nH_2)$ (n=1–5) are optimized using MP2 [25] method. Becke's three parameter hybrid functional combined with the Lee, Yang, and Parr correlation (B3LYP) functional, the 1996 and 1997 gradient-corrected correlation functional of Perdew, Burke and Ernzerhof (PBE) and a pure standalone functional constructed with a long range dispersion correction of Grimme (B97D) are also used for the geometry optimization [26–31]. An all-electron DGauss double-zeta valence polarization (DGDZVP) basis set has been used. The MD simulations were carried out using ADMP [32]. The time step (Δt) of the ADMP-MD was set at 0.2 fs, and temperature was maintained using the velocity scaling method during the MD simulations. All calculations were performed using the Gaussian 03 suite of programs [33]. The geometry optimization and MD simulations carried out using B97D were performed using the Gaussian 09 suite of programs [34]. Many-body analysis technique has been used to obtain various interaction energies in a complex and to study the nature of interactions between H_2 molecule and C_3Ti/C_3Ti^+ cluster and that between H_2 molecules within a complex [35–38]. The basis set superposition error (BSSE) corrected total energy was obtained by the method suggested by Valiron and Mayer [39].

Results and discussion

First we optimized the geometries of $C_3Ti(4H_2)$ and $C_3Ti^+(5H_2)$ using MP2 and different DFT method. Maximum four H_2 molecules can be adsorbed on C_3Ti whereas five on C_3Ti^+ at all the levels used here. This shows the gravimetric H_2 uptake capacity of 8.77 and 10.73 wt% for C_3Ti and C_3Ti^+, respectively. The ionization has enhanced

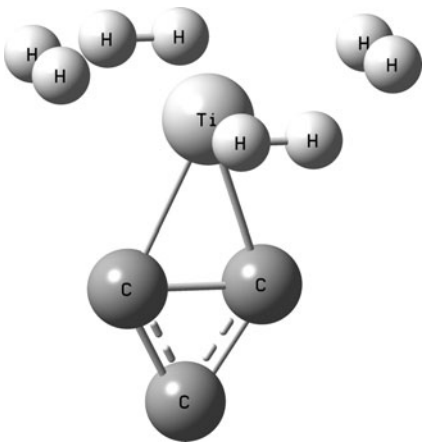

Fig. 1 Optimized geometry of $C_3Ti(4H_2)$ complex using MP2 method

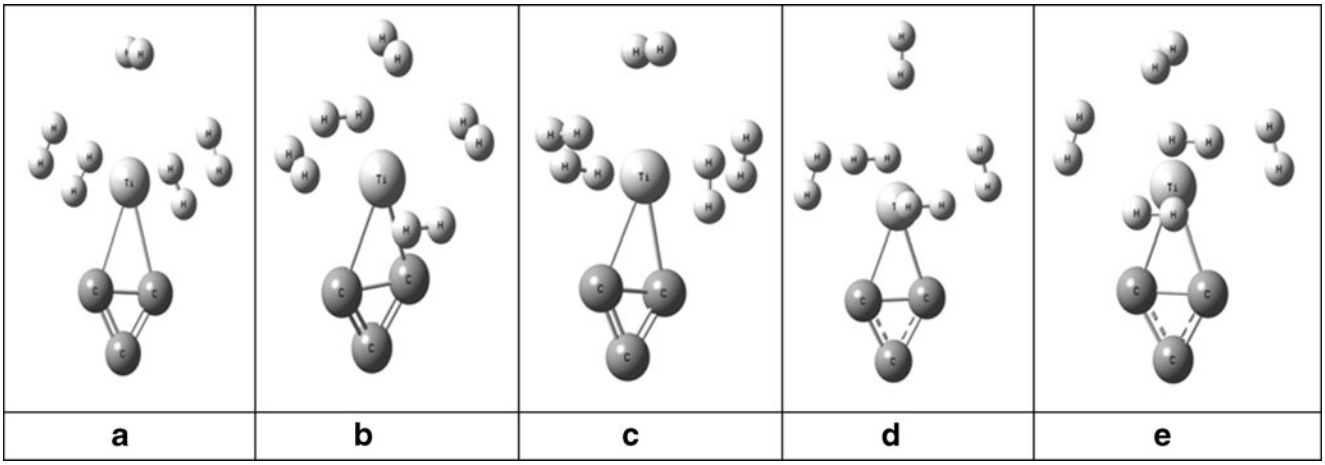

Fig. 2 Optimized geometries of $C_3Ti^+(5H_2)$ complexes using (**a**) MP2 (**b**) B3LYP (**c**) PBE0 (**d**) PBE (**e**) B97D method

the hydrogen uptake capacity of C_3Ti complex by about 2 wt %. The first H_2 molecule was adsorbed nondissociatively on C_3Ti using DFT methods whereas it was adsorbed in dihydride form using the MP2 method. All the methods used here have produced identical final geometry of $C_3Ti(4H_2)$ as shown in Fig. 1. The distance between H_2 molecules and Ti in $C_3Ti(4H_2)$ is in the range of 1.96–1.99, 1.95–1.98, 1.93–1.95 and 1.92–1.94, 1.95–1.98 Å using MP2, B3LYP, PBE0, PBE and B97D methods respectively. The bond length between the carbon atoms to which Ti is attached gets shortened when the maximum numbers of H_2 molecules are adsorbed on it using DFT methods whereas for the MP2 method the opposite is true. No large change in the C-C length is observed after the adsorption of H_2 molecules on the C_3Ti complex using B97D method. On the other hand, the C-Ti bond is shortened (elongated) by MP2 (DFT) method than that in isolated C_3Ti complex. Unlike $C_3Ti(4H_2)$, $C_3Ti^+(5H_2)$ does not have the same final optimized geometry obtained using different methods. The geometries of $C_3Ti^+(5H_2)$ are shown in Fig. 2. The Ti-H_2 distance in $C_3Ti^+(5H_2)$ is in the range of 2.26-2.43, 2.03-2.44, 2.09-2.21 and 2.11-3.36 Å at MP2, B3LYP, PBE0 and PBE level, respectively. This indicates that the H_2 molecules bound strongly to C_3Ti than C_3Ti^+ and lie at a longer distance in $C_3Ti^+(5H_2)$ than those in $C_3Ti(4H_2)$ complex. The H-H distances in $C_3Ti(4H_2)$ are slightly longer than that for the isolated H_2 molecule whereas in $C_3Ti^+(5H_2)$ those are very close to the H-H equilibrium distance.

The HOMO-LUMO gap for the $C_3Ti(nH_2)$ (n=1–4) and $C_3Ti^+(nH_2)$ (n=1–5) complexes with successive addition of H_2 molecules is shown in Fig. 3. If the HOMO-LUMO gap of a complex is higher it indicates that the further reactivity of that complex is lower. The HOMO-LUMO gap for the H_2 adsorbed C_3Ti complex is larger than that for the isolated C_3Ti structure indicating more kinetic stability of $C_3Ti(4H_2)$ complex. $C_3Ti(nH_2)$ structures are kinetically more stable than the $C_3Ti^+(nH_2)$ for all n since at all level the gap predicted for the $C_3Ti^+(nH_2)$ is lower than that for the $C_3Ti(nH_2)$ complex. The HOMO-LUMO gap predicted by all the DFT methods increase gradually when successive H_2 molecules are added to the C_3Ti complex. As can be

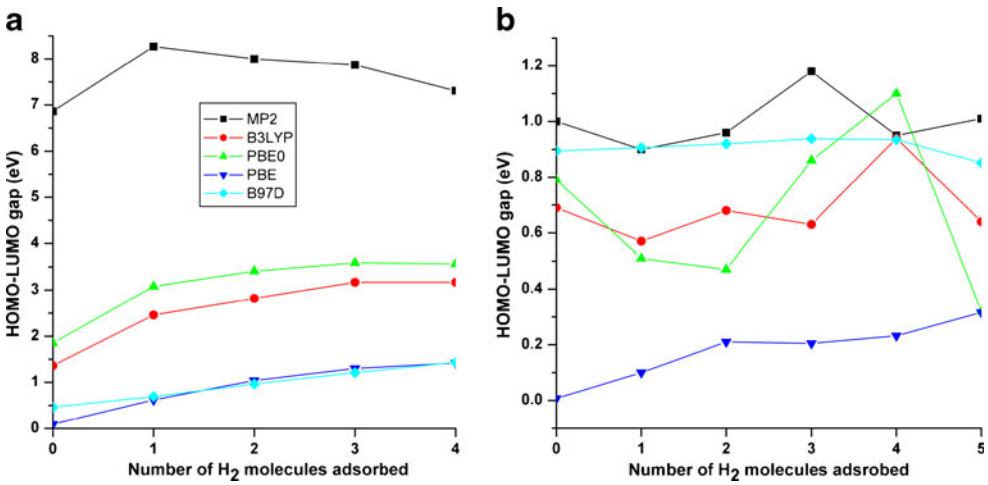

Fig. 3 Energy gap between highest occupied and lowest unoccupied molecular orbital for (**a**) $C_3Ti(4H_2)$ (n=1–4) and (**b**) $C_3Ti^+(5H_2)$ (n=1–5) complexes with successive addition of H_2 molecule. (Color online)

Table 1 Selected vibrational modes (in cm^{-1}) of $C_3Ti(4H_2)$ and $C_3Ti^+(5H_2)$ complexes using different methods with DGDZVP basis set. The values in the paranthesis are for $C_3Ti^+(5H_2)$ complex

Assignments	Ti-H_2 stretch (symmetric)	Ti-H_2 stretch (asymmetric)	H-H stretch
MP2	677/719/847/909	1303/1321/1391/1442	3235/3346/3465/3561
	(353/454/415/433/476)	(551/631/632/710/715)	(4355/4377/4378/4386)
B3LYP	(352/576/653/654/712)	(530/1011/1035/1073/1108)	(3825/3849/3938/3964/4334)
	672/750/792/854	1236/1264/1314/1368	3276/3367/3484/3557
PBE0	707/794/856/906/919	1316/1345/1386/1437	3148/3245/3340/3425
	(523/569/588/598/646)	(777/855/860/909/933)	(4082/4088/4139/4149/4152)
PBE	704/805/851/900/928	1308/1345/1387/1435	2900/3009/3122/3212
	(591/595/610/626)	(856/870/909/911)	(3926/3929/3983/3993/4229)
B97D	762/767/859/825	1185/1216/1319/1375	3129/3233/3369/3450
	(342/387/409/422/465)	(687/735/737/744)	(4117/4129/4133/4144/4330)

seen from Fig. 3a, a rise in the gap for n=1 is observed and then it decreases for n=2 and remains nearly constant afterward for the MP2 method. It is due to the fact that, in $C_3Ti(1H_2)$ complex the H_2 molecule is adsorbed by chemisorption and hence for further reactivity a barrier of somewhat more energy is to be crossed. The gap predicted by the B97D method when successive H_2 molecules are added to the C_3Ti complex is almost equal to that obtained by using the GGA method. There is no rising trend observed when the H_2 molecules are added to the C_3Ti^+ complex for all methods except GGA because the formation of most of the complexes is endothermic and hence thermodynamically unstable. The thermodynamic stability of these complexes is discussed latter in the text.

Vibrational modes for $C_3Ti(4H_2)$ and $C_3Ti^+(5H_2)$ complexes are represented in Table 1. There are no imaginary frequencies to $C_3Ti(4H_2)$ as well as $C_3Ti^+(5H_2)$ complexes indicating that both the structures are quantum mechanically stable. The modes given in Table 1 viz. Ti-H_2 symmetric/asymmetric and H-H stretching are the only high intensity modes observed in these complexes.

The adsorption energies for the $C_3Ti(nH_2)$ (n=1–4) and $C_3Ti^+(nH_2)$ (n=1–5) at different levels of theories are represented in Table 2. The adsorption energy per H_2 molecule without Gibbs free energy correction is calculated for each structure as

$$\Delta E = \{E[C_3M] + E[nH_2] - E[C_3M(nH_2)]\}/n, \quad (1)$$

where *E[X]* is the total energy of *X* and *M* represents either Ti or Ti^+.

The adsorption energy obtained is higher for GGA functional > hybrid DFT functional > MP2 for C_3Ti and C_3Ti^+. This shows the dependence of adsorption energy on the computational level used. It is generally observed that GGA functional predicts higher adsorption energy than the hybrid DFT functionals. Also in hybrid DFT functional, PBE0 gives larger adsorption energies than the B3LYP as former contains 25 % Hartree Fock (HF) contribution where as latter 20 %. More the HF contribution the higher the adsorption energy. This is normally considered as an effect of exchange and correlation functional on the adsorption energy. Effect of exchange and correlation functional on adsorption energy was also reported earlier [40, 41]. The adsorption energy per H_2 molecule with Gibbs free energy correction (ΔE_G) is calculated as concise

$$\Delta E_G = \{E_G[C_3M] + E_G[nH_2] - E_G[C_3M(nH_2)]\}/n, \quad (2)$$

Table 2 Calculated adsorption energies per H_2 molecule with zero point energy correction (ΔE) and adsorption Gibbs free energy (in parenthesis) in eV at 298.15 K for $C_3Ti(nH_2)$ (n=1–4) and $C_3Ti^+(nH_2)$ (n=1–5) complex using different levels of theories

Complex	ΔE (ΔE_G)				
	MP2	B3LYP	PBE0	PBE	B97D
$C_3Ti(1H_2)$	1.26 (0.99)	0.62 (0.34)	0.72 (0.45)	0.55 (0.26)	0.48(0.19)
$C_3Ti^+(1H_2)$	0.13 (−0.09)	0.24 (−0.01)	0.27 (0.05)	0.33 (0.09)	0.23(−0.02)
$C_3Ti(2H_2)$	0.45 (0.17)	0.43 (0.15)	0.60(0.31)	0.63 (0.34)	0.42(0.12)
$C_3Ti^+(2H_2)$	0.13 (−0.10)	0.21 (−0.04)	0.25 (0.02)	0.31 (0.07)	0.23(−0.02)
$C_3Ti(3H_2)$	0.38 (0.09)	0.43 (0.15)	0.51 (0.23)	0.55 (0.26)	0.37(0.08)
$C_3Ti^+(3H_2)$	−0.10 (−0.35)	0.22 (−0.04)	0.25 (−0.01)	0.31 (0.04)	0.26(−0.01)
$C_3Ti(4H_2)$	0.35 (0.05)	0.39 (0.10)	0.48 (0.18)	0.51 (0.22)	0.34(0.05)
$C_3Ti^+(4H_2)$	0.11 (−0.14)	0.21 (−0.06)	0.25 (−0.02)	0.30 (0.03)	0.25(−0.02)
$C_3Ti^+(5H_2)$	−0.03 (−0.28)	0.10 (−0.18)	0.21 (−0.06)	0.25 (−0.01)	0.21(−0.06)

where $E_G[X]$ stands for the energy of X with Gibbs free energy correction.

The ΔE_G values are positive for $C_3Ti(nH_2)$ (n=1–4) using all the methods used here which indicate that the adsorption of four H_2 molecules on C_3Ti is exothermic at room temperature. The higher ΔE value of 1.26 eV for the $C_3Ti(1H_2)$ complex is because of the adsorption of H_2 molecule in dihydride from. Other than this, the DFT calculated adsorption energies are not much off from the MP2 values. For $C_3Ti^+(nH_2)$ (n=1–5), H_2 adsorption is endothermic using B3LYP, B97D and MP2 method for all n. The H_2 adsorption is exothermic and endothermic for n=1–2 and n=3–5 respectively for $C_3Ti^+(nH_2)$ at PBE0 level. Using PBE method, adsorption of H_2 molecule on C_3Ti^+ is energetically favorable for n=1–4 whereas it is unfavorable for n=5.

In Table 3 BSSE corrected many-body energies are represented at B3LYP/DGDZVP level. The contribution from the relaxation energy and many-body energies viz. two-, three-, four-, five- and six-body to the binding energy

Table 3 BSSE corrected many-body interaction energies, total many-body energies and binding energy for $C_3Ti(4H_2)$ and $C_3Ti^+(5H_2)$ complex at B3LYP/DGDZVP level

Interaction energy term	Energy(kcal/mol)		Interaction energy term	Energy(kcal/mol)	
	$C_3Ti(4H_2)$	$C_3Ti^+(5H_2)$		$C_3Ti(4H_2)$	$C_3Ti^+(5H_2)$
Two-body					
OM-H1	−18.23	−6.00	H2-H4-H5	——	−0.13
OM-H2	−15.19	−4.27	H3-H4-H5	——	−0.05
OM-H3	−18.23	3.63	Four-body		
OM-H4	−15.19	2.93	OM-H1-H2-H3	−1.15	19.74
OM-H5	——	3.65	OM-H1-H2-H4	−1.66	14.73
H1-H2	1.19	0.29	OM-H1-H2-H5	——	2.16
H1-H3	0.01	0.56	OM-H1-H3-H4	−1.15	10.05
H1-H4	1.19	0.05	OM-H1-H3-H5	——	5.34
H1-H5	——	0.56	OM-H1-H4-H5	——	2.42
H2-H3	1.19	0.89	OM-H2-H3-H4	−1.66	19.43
H2-H4	0.10	0.29	OM-H2-H3-H5	——	9.13
H2-H5	——	0.84	OM-H2-H4-H5	——	−1.06
H3-H4	1.19	0.57	OM-H3-H4-H5	——	5.0
H3-H5	——	0.06	H1-H2-H3-H4	0.23	0.02
H4-H5	——	0.56	H1-H2-H3-H5	——	0.04
Three-body			H1-H2-H4-H5	——	0.02
OM-H1-H2	−0.004	−2.02	H1-H3-H4-H5	——	0.06
OM-H1-H3	6.34	−10.18	H2-H3-H4-H5	——	0.04
OM-H1-H4	−0.004	−5.19	Five-body		
OM-H1-H5	——	−1.67	OM-H1-H2-H3-H4	−0.85	−29.70
OM-H2-H3	−0.003	−7.79	OM-H1-H2-H3-H5	——	−14.98
OM-H2-H4	6.71	−10.94	OM-H1-H2-H4-H5	——	−0.82
OM-H2-H5	——	1.42	OM-H1-H3-H4-H5	——	−1.63
OM-H3-H4	−0.004	−9.87	OM-H2-H3-H4-H5	——	−3.45
OM-H3-H5	——	−8.60	H1-H2-H3-H4-H5	——	−0.01
OM-H4-H5	——	−10.60	Six-body		
H1-H2-H3	−0.15	−0.13	OM-H1-H2-H3-H4-H5	——	−3.05
H1-H2-H4	−0.14	−0.02	$E_{Relaxation}$	4.44	0.69
H1-H2-H5	——	−0.13	Total two-body	−61.87	4.64
H1-H3-H4	−0.15	−0.05	Total three-body	12.45	−66.24
H1-H3-H5	——	−0.05	Total four-body	−5.39	87.15
H1-H4-H5	——	−0.05	Total five-body	−0.85	−50.59
H2-H3-H4	−0.14	−0.13	Total six-body	——	−3.05
H2-H3-H5	——	−0.06	B.E.	−51.21	−27.40

of $C_3Ti(4H_2)$ and $C_3Ti^+(5H_2)$ complexes can be clearly seen from Table 3. In Table 3, OM represents the organometallic complex either C_3Ti or C_3Ti^+ and Hi represents the i^{th} hydrogen molecule in a H_2 adsorbed complex. In $C_3Ti(4H_2)$ complex, all OM-Hi interactions are attractive in nature whereas all Hi-Hj (i≠j) interactions are repulsive. The three-, four- and five-body interactions are attractive except the OM-H1-H3 and OM-H2-H4 interactions in $C_3Ti(4H_2)$ complex. The nature of total two-, four- and five-body interactions is attractive whereas the total three-body interaction is repulsive for this complex. The major contribution to the binding energy of $C_3Ti(4H_2)$ complex is from the total two-body interaction. In $C_3Ti^+(5H_2)$, all the two-body interactions are repulsive except the OM-H1 and OM-H2 interactions which are of attractive nature. All the three-, five- and six-body interactions are attractive. Among the 15 four-body interactions only OM-H2-H4-H5 interaction is attractive. Total three-body and total five-body energies have major contribution to the binding energy of $C_3Ti^+(5H_2)$ complex. The binding energy calculated using many-body analysis technique for $C_3Ti(4H_2)$ and $C_3Ti^+(5H_2)$ complex is −51.21 and −27.40 kcal mol^{-1} respectively whereas it is −51.27 and −27.42 kcal mol^{-1} calculated using the supramolecular approach. For both the complexes, many-body energies for those interaction terms containing only H_2 molecules are negligible as compared to those containing organometallic complex as one of the many-body terms. This indicates that in this case the BSSE is very small.

The trend observed for the Mulliken and natural atomic charge on Ti/Ti^+ in C_3Ti/C_3Ti^+ is MP2>B3LYP>PBE0>PBE. These charges decrease with successive addition of H_2 molecules on C_3Ti as well as C_3Ti^+ for all the levels. More the negative Mulliken charge on Ti, higher is the H_2 adsorption energy. Most of the negative charge is localized on the carbon atoms to which Ti/Ti^+ atom is attached whereas most of the positive charge is localized on Ti/Ti^+ atom in $C_3Ti(4H_2)$/ $C_3Ti^+(5H_2)$. When maximum numbers of H_2 molecules are adsorbed on C_3Ti/C_3Ti^+ positive charge from Ti and negative charge from C is transferred to the H_2 molecules. The natural charge on carbon atoms is more negative at MP2>B3LYP>PBE0>PBE method. The positive charge on Ti in C_3Ti and C_3Ti^+ is responsible for the binding of H_2 molecules. The interaction between transition metal (TM) and H_2 molecule has already been explained which is well known as Kubas interaction [42, 43]. It explains the forward donation of the bonding electron of H_2 to partially filled *d* orbital of TM and back donation from TM to antibonding orbital of H_2.

We have also studied the effect of temperature on ΔE_G to obtain the temperature range for which 'n' hydrogen molecule adsorption is energetically favorable on C_3Ti and C_3Ti^+ for all the levels of theories and is shown in Fig. 4. As can be seen from Fig. 4 the adsorption of four H_2 molecules on C_3Ti is thermodynamically possible below temperatures 344, 380, 446, 473, 349 K with MP2, B3LYP, PBE0, PBE and B97D calculations, respectively. In the case of C_3Ti^+, the adsorption of five H_2 molecules is not thermodynamically possible at room temperature for all the levels used here. The adsorption of five H_2 molecules is not energetically favorable unless the temperature is very low using the MP2 method. The adsorption of five H_2 molecules on C_3Ti^+ is favorable below 130, 280, 243 and 235 K on C_3Ti^+ using B3LYP, PBE, PBE0 and B97D methods, respectively. The ΔE_G values calculated using pure functional B97D nearly overlap with the MP2 and PBE0 values for $C_3Ti(4H_2)$ and $C_3Ti^+(5H_2)$ complex respectively.

ADMP-MD simulations are carried out to study the H_2 adsorption phenomenon on C_3Ti and C_3Ti^+ at room temperature. The trajectories of time evolution of distance between center of mass of H_2 molecules and Ti denoted by R_{H2} in $C_3Ti(4H_2)$ and $C_3Ti^+(5H_2)$ complexes are examined using hybrid DFT (B3LYP), GGA (PBE), B97D and MP2 methods. The outcome of MD simulation differs from each other using different methods. The trajectories of R_{H2} using

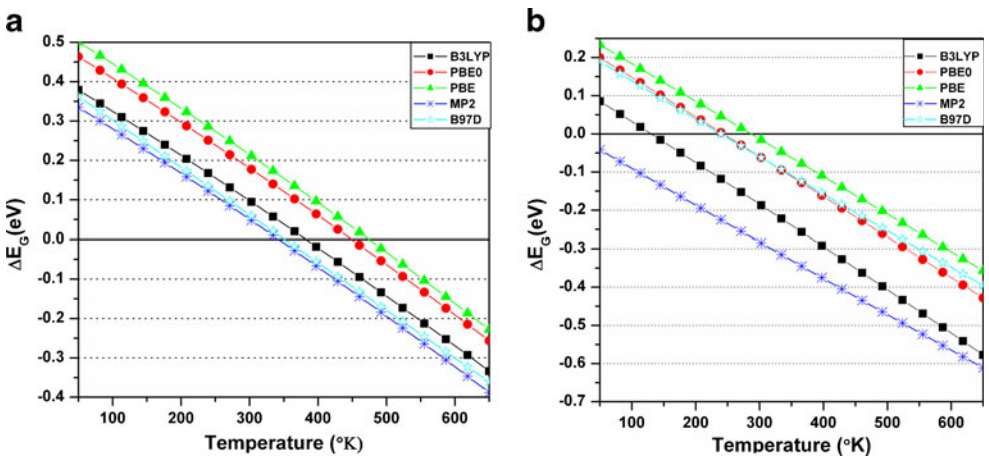

Fig. 4 Temperature dependence of averaged H_2 adsorption Gibbs free energy for (**a**) $C_3Ti(4H_2)$ and (**b**) $C_3Ti^+(5H_2)$ complexes. (Color online)

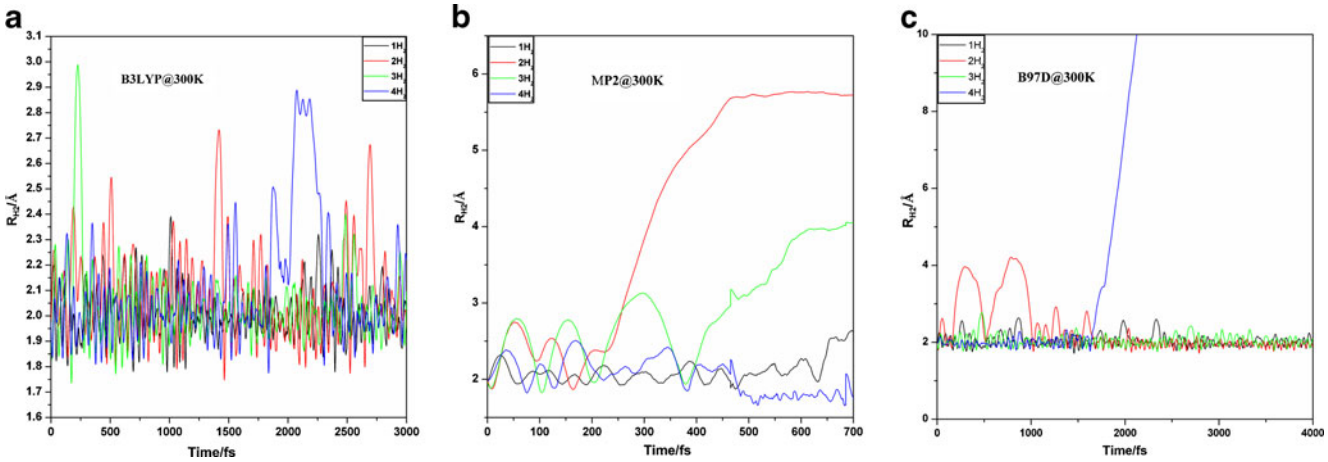

Fig. 5 Trajectories of time evolution of R_{H2} in $C_3Ti(4H_2)$ complex at T=300 K calculated using ADMP-MD with the (**a**) B3LYP (**b**) MP2 (**c**) B97D method. (Color online)

B3LYP method at T=300 K are shown in Fig. 5a. We found that four H_2 molecules remain adsorbed on C_3Ti within 3 ps. The R_{H2} of four H_2 molecules oscillate around 2 Å within 3 ps. Similar ADMP-MD results are obtained using PBE method. Results from the ADMP-MD simulation using MP2 method are shown in Fig. 5b which differs from those obtained using the hybrid and GGA functional in DFT. As shown in Fig. 5b, two molecules get desorbed from C_3Ti whereas two remain adsorbed on it at room temperature. Out of two adsorbed molecules, one gets dissociated and adsorbed in atomic form. Out of the two desorbed molecules, first get desorbed at around 0.25 ps and second at 0.45 ps. As shown in Fig. 5c, when simulation is carried out using B97D method, it is found that three molecules oscillate around 2 Å at room temperature up to 4 ps and one molecule get desorbed from C_3Ti complex after 1.5 ps.

Figure 6a, b and c shows the time evolution of R_{H2} in $C_3Ti^+(5H_2)$ using ADMP-MD simulation with PBE, B3LYP and B97D methods, respectively. ADMP-MD simulations with PBE method show that four H_2 molecules are adsorbed on C_3Ti^+ and oscillates around 2 Å within 1 ps and one H_2 molecule gets desorbed from C_3Ti^+ as shown in Fig. 6a. Three molecules are adsorbed and two are desorbed on C_3Ti^+ when ADMP-MD simulations are carried out using B3LYP method as shown in Fig. 6b. Three adsorbed molecules oscillate around 2.5 Å and the adsorption is completely molecular. The ADMP-MD simulations with MP2 method show that, not a single molecule is adsorbed on C_3Ti^+ and the C_3Ti^+ structure collapses too. MD simulation results using B97D reveals similar results as that obtained using PBE method. Four H_2 molecules are adsorbed to $C3Ti^+$ complex and one gets desorbed from it during the simulations at 300 K. In the insect the trajectories of the four H_2 molecules oscillating around 2.4 Å is shown and the trajectory of the 3rd H_2 molecule which is desorbed from $C3Ti^+$ complex is excluded.

The hydrogen storage capacity of Ti-decorated carbon ring structures like C_4H_4, C_5H_5, C_6H_6 and also C_8H_8 have been reported earlier [44, 45]. It was reported that the complexes like C_4H_4Ti, C_5H_5Ti, C_6H_6Ti and C_8H_8Ti can adsorb up to five, four, four and three H_2 molecules

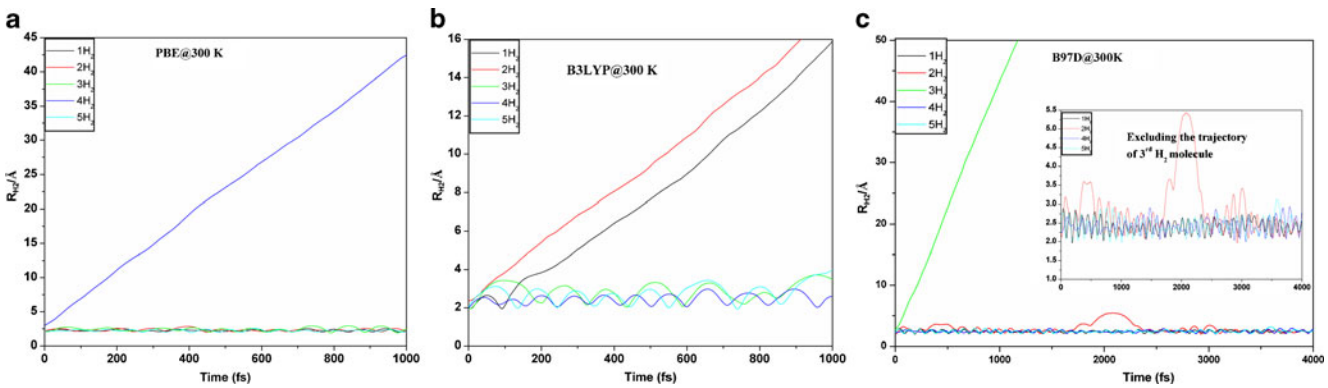

Fig. 6 Trajectories of time evolution of R_{H2} in $C_3Ti^+(5H_2)$ complex at T=300 K calculated using ADMP-MD with the (**a**) PBE (**b**) B3LYP (**c**) B97D method. (Color online)

respectively. In these structures, first H_2 molecule is adsorbed dissociatively and remains in dihydride form till the introduction of the third, third and second H_2 molecule on C_4H_4Ti, C_5H_5Ti and C_6H_6Ti respectively. On C_3Ti and C_3Ti^+ the H_2 adsorption is nondissociative for all n with different methods used here except for $C_3Ti(1H_2)$ using the MP2 method. C_3Ti and C_3Ti^+ give the gravimetric H_2 uptake capacity which meets the target specified by the United States (US) department of energy (DOE) (6 wt % by 2010). Only C_4H_4Ti meets the target of DOE among the above mentioned Ti decorated ring structures.

We suggest C_3Ti as suitable material for the hydrogen storage than C_3Ti^+ since

i) Its hydrogen uptake capacity is 8.77 wt % which meets the target specified by the DOE. This is confirmed by the ADMP-MD simulations using DFT method. Though the H_2 uptake capacity of C_3Ti^+ is higher than that of C_3Ti, adsorption Gibbs free energy shows that H_2 adsorption is energetically unfavorable on C_3Ti^+.
ii) The H_2 adsorption on C_3Ti is energetically favorable for wide range of temperature including room temperature than that on C_3Ti^+. This is true for all the levels of theory used here.
iii) The kinetic stability of a four H_2 adsorbed C_3Ti complex is confirmed by the HOMO-LUMO gap. $C_3Ti(4H_2)$ complex has large HOMO-LUMO gap at all the levels of theories used here.
iv) Even after four H_2 molecules adsorption on C_3Ti, Ti remains strongly bound to C_3. This is confirmed by the binding energy between C_3 and Ti before and after H_2 adsorption.
v) There is a strong attractive interaction between C_3Ti and adsorbed H_2 molecules. This is confirmed by obtaining OM-Hi interaction energies using many-body analysis approach.

Conclusions

Ab initio and DFT calculations revealed that structures like C_3Ti in which transition metal is tightly bound to the system can bind four H_2 molecules. The C_3Ti molecule shows the gravimetric hydrogen uptake capacity 8.77 wt %. The hydrogen adsorption energies depend on the level of theory used in computation. Thermo-chemistry studies using different methods have shown that adsorption of four H_2 molecules is possible at room temperature on C_3Ti. Though C_3Ti^+ adsorbs one additional H_2 molecule than C_3Ti, H_2 adsorption energies for the former are not energetically favorable. ADMP-MD simulations at temperature 300 K have shown that C_3Ti can adsorb four and two H_2 molecules at DFT and MP2 level, respectively. C_3Ti complex is a more promising material for hydrogen storage than C_3Ti^+. It is also dominating over single Ti atom decorated ring structures in regard with hydrogen storage. Many-body analysis of the H_2 adsorbed complex shows that higher interaction terms are not negligible and contribute significantly to the binding energy of a respective complex.

Acknowledgments The Financial support from Council for Scientific and Industrial Research, New Delhi (Grant no. 03(1115)/08/EMR-II) and Swami Ramanand Teerth Marathwada University in terms of university funded research fellowship is gratefully acknowledged.

References

1. Schlapbach L, Zuttel A (2001) Nature (Lond) 414:353–358
2. Coontz R, Hanson B (2004) Science 305:957–957
3. Dillon AC, Jones KM, Bekkendahl TA, Kiang CH, Bethune DS, Hebe MJ (1997) Nature (Lond) 386:377–379
4. Chan SP, Chen G, Gong XG, Liu ZF (2001) Phys Rev Lett 87:205502(1–4)
5. Tada K, Furuya S, Watanabe K (2001) Phys Rev B 63:155405(1–4)
6. Dubot P, Cenedese P (2001) Phys Rev B 63:241402(1–4)
7. Gulseren O, Yildirim T, Ciraci S (2001) Phys Rev Lett 87:116802(1–4)
8. Lee EC, Kim YS, Jin YG, Chang KJ (2002) Phys Rev B 66:073415(1–4)
9. Lu G, Scudder H, Kioussis N (2003) Phys Rev B 68:205416(1–5)
10. Miura Y, Kasai H, Dino WA, Nakanishi H, Sugimoto T (2003) J Appl Phys 93:3395(1–6)
11. Deng WQ, Xu X, Goddard WA (2004) Phys Rev Lett 92:166103(1–4)
12. Dag S, Ozturk Y, Ciraci S, Yildirim T (2005) Phys Rev B 72:155404(1–8)
13. Yildirim T, Ciraci S (2005) Phys Rev Lett 94:175501(1–4)
14. Zhao Y, Kim YH, Dillon AC, Heben MJ, Zhang SB (2005) Phys Rev Lett 94:155504(1–4)
15. Yildirim T, Iniguez J, Ciraci S (2005) Phys Rev B 72:153403(1–4)
16. Bogdanovic B, Felderhoff M, Kaskel S, Pommerin A, Schlichte K, Schuth F (2003) Adv Mater (Weinheim, Ger) 15:1012–1015
17. Yildirim T, Hartman MR (2005) Phys Rev Lett 95:215504(1–4)
18. Zhao Y, Dillon AC, Kim YH, Heben MJ, Zhang SB (2006) Chem Phys Lett 425:273–277
19. Akman N, Durgun E, Yildrim T, Ciraci S (2006) Hydrogen J Phys: Condens Matter 18:9509–9517
20. Lee H, Choi WI, Ihm J (2006) Phys Rev Lett 97:056104(1–4)
21. Gagliardi L, Pyykko P (2004) J Am Chem Soc 126:15014–15015
22. Phillips AB, Shivaram BS (2008) Phys Rev Lett 100:105505(1–4)
23. Wang XB, Ding CF, Wang LS (1997) J Phys Chem A 101:7699–7701
24. Okamoto Y, Miyamoto Y (2001) J Phys Chem B 105:3470–3474
25. Møller C, Plesset MS (1934) Phys Rev 46:618–622
26. Becke AD (1988) Phys Rev A 38:3098–3100
27. Becke AD (1993) J Chem Phys 98:5648–5652
28. Becke AD (1997) J Chem Phys 107:8554–8560
29. Perdew JP, Burke K, Ernzerhof M (1996) Phys Rev Lett 77:3865–3868
30. Perdew JP, Burke K, Ernzerhof M (1997) Phys Rev Lett 78:1396–1396
31. Grimme S (2006) J Comput Chem 27:1787–1799
32. Schlegel HB, Iyengar SS, Li X, Millam JM, Voth GA, Scuseria GE, Frisch MJ (2002) J Chem Phys 117:8694–8704
33. Frisch MJ, Trucks GW, Schlegel HB, Scuseria GE, Robb MA, Cheeseman JR, Montgomery JA, Vreven T, Kudin KN, Burant JC, Millam JM, Iyengar SS, Tomasi J, Barone V, Mennucci B, Cossi M, Scalmani G, Rega N, Petersson GA, Nakatsuji H, Hada

M, Ehara M, Toyota K, Fukuda R, Hasegawa J, Ishida M, Nakajima T, Honda Y, Kitao O, Nakai H, Klene M, Li X, Knox JE, Hratchian HP, Cross JB, Bakken V, Adamo C, Jaramillo J, Gomperts R, Stratmann RE, Yazyev O, Austin AJ, Cammi R, Pomelli C, Ochterski JW, Ayala PY, Morokuma K, Voth GA, Salvador P, Dannenberg JJ, Zakrzewski VG, Dapprich S, Daniels AD, Strain MC, Farkas O, Malick DK, Rabuck AD, Raghavachari K, Foresman JB, Ortiz JV, Cui Q, Baboul AG, Clifford S, Cioslowski J, Stefanov BB, Liu G, Liashenko A, Piskorz P, Komaromi I, Martin RL, Fox DJ, Keith T, Al-Laham MA, Peng CY, Nanayakkara A, Challacombe M, Gill PMW, Johnson B, Chen W, Wong MW, Gonzalez C, Pople JA (2004) Gaussian 03. Gaussian Inc, Wallingford, CT

34. Frisch MJ, Trucks GW, Schlegel HB, Scuseria GE, Robb MA, Cheeseman JR, Scalmani G, Barone V, Mennucci B, Petersson GA, Nakatsuji H, Caricato M, Li X, Hratchian HP, Izmaylov AF, Bloino J, Zheng G, Sonnenberg JL, Hada M, Ehara M, Toyota K, Fukuda R, Hasegawa J, Ishida M, Nakajima T, Honda Y, Kitao O, Nakai H, Vreven T, Montgomery JA, Peralta JE, Ogliaro F, Bearpark M, Heyd JJ, Brothers E, Kudin KN, Staroverov VN, Kobayashi R, Normand J, Raghavachari K, Rendell A, Burant JC, Iyengar SS, Tomasi J, Cossi M, Rega N, Millam NJ, Klene M, Knox JE, Cross JB, Bakken V, Adamo C, Jaramillo J, Gomperts R, Stratmann RE, Yazyev O, Austin AJ, Cammi R, Pomelli C, Ochterski JW, Martin RL, Morokuma K, Zakrzewski VG, Voth GA, Salvador P, Dannenberg JJ, Dapprich S, Daniels AD, Farkas U, Foresman JB, Ortiz JV, Cioslowski J, Fox DJ (2009) Gaussian 09, Revision A.1. Gaussian Inc, Wallingford CT
35. Xantheas SS (1994) J Chem Phys 100:7523–7534
36. Xantheas SS (1995) J Chem Phys 102:4505–4517
37. Chaudhari A, Sahu PK, Lee SL (2004) J Chem Phys 120:170–174
38. Chaudhari A, Lee SL (2004) J Chem Phys 120:7464–7469
39. Valiron P, Mayer I (1997) Chem Phys Lett 275:46–55
40. Okamoto Y (2008) J Phys Chem C 112:17721–17725
41. Kalamse V, Wadnerkar N, Chaudhari A (2010) J Phys Chem C 114:4704–4709
42. Kubas GJ, Ryan RR, Swanson BI, Vergamini PJ, Wasserman HJ (1984) J Am Chem Soc 106:451–452
43. Kubas GJ (2001) Metal dihydrogen and σ-bond complexes. Kluwer, New York,
44. Weck PF, Dhilip Kumar TJ (2007) J Chem Phys 126:094703–094706
45. Kiran B, Kandalam AK, Jena P (2006) J Chem Phys 124:224703–224706